A mathematical model for light dosimetry in photodynamic destruction of human endometrium

1996 Phys. Med. Biol. 41 223

(http://iopscience.iop.org/0031-9155/41/2/002)

Phys. Med. Biol. **41** (1996) 223–237. Printed in the UK

A mathematical model for light dosimetry in photodynamic destruction of human endometrium

Bruce J Tromberg†, Lars O Svaasand†‡, Mathias K Fehr†§,
Steen J Madsen†, Pius Wyss†§, Beverly Sansone‖ and Yona Tadir†‖

† Beckman Laser Institute and Medical Clinic, University of California, Irvine, CA 92715, USA
‡ Norwegian Institute of Technology, 7034 Trondheim, Norway
§ Department of Obstetrics and Gynecology, University of Zürich, 8091 Zürich, Switzerland
‖ Department of Obstetrics and Gynecology, University of California, Irvine, CA 92715, USA

Received 29 September 1994, in final form 30 October 1995

Abstract. We are involved in the development of photodynamic therapy (PDT) as a minimally invasive method for treating dysfunctional uterine bleeding, one of the primary clinical indications for hysterectomy. In this paper, we analyse light propagation through the uterus in order to specify the requirements for a light delivery system capable of effectively performing endometrial PDT. Our approach involves developing an analytical model based on diffusion theory to predict optical fluence rate distributions when cylindrical and spherical optical applicators are placed in the uterine cavity. We apply the results of our model calculations to estimate the thermal effects of optical irradiation and the effective photodynamic optical dose. Theoretical fluence rate calculations are compared to fluence rate measurements made in fresh, surgically removed human uteri.

Our results show that a trifurcated cylindrical optical applicator inserted into the human uterus can provide a light dose that is sufficient to cause photodynamic destruction of the entire endometrium. When the optical power per unit length of each cylindrical applicator is 100 mW cm^{-1} (at 630 nm), a fluence rate of 40 mW cm^{-2} is delivered to the boundary layer between the endometrium and the myometrium (a depth of about 4–6 mm). The optical fluence delivered to the boundary layer after 20 min of exposure is 50 J cm^{-2}, a level that is generally accepted to cause tissue damage throughout the endometrium in most patients.

1. Introduction

Surgical removal of the uterus (hysterectomy) is the most common major operation in the United States, and dysfunctional uterine bleeding is one of the primary clinical indications for surgical intervention. The procedure is performed on an estimated 600 000 patients each year (Lynne *et al* 1994).

Endometrial ablation has long been recognized as an alternative to hysterectomy for abnormal uterine bleeding produced by benign changes in physiology. Unfortunately, attempts to develop medical and surgical ablation techniques have, thus far, yielded imperfect results. For example, routinely performed, minimally invasive surgical procedures, such as hysteroscopic Nd:YAG laser ablation (Goldrath *et al* 1981) and electrocautery with a rollerball or resectoscope (Daniel *et al* 1992, DeCherney and Polan 1983, Serden and Brooks 1991) are associated with specific risks. These include perforation, bleeding, cervical stenosis, coagulopathy, fluid overload, and air embolism (DeCherney and Polan 1983, Brooks and Serden 1991, Jedeikin *et al* 1990, Perry and Baughman 1990).

0031-9155/96/020223+15$19.50

Moreover, these surgical techniques require general anaesthesia and hospitalization for a period of at least 24 h.

In contrast to conventional tissue destruction methods, we have been involved in the application of a well known photochemical method, photodynamic therapy (PDT), as a minimally invasive modality for endometrial destruction. Our goal is to optimize PDT since it can cause selective destruction of the endometrium without the risks of anaesthesia or the costs of hospitalization. Studies in rats and rabbits clearly show that various photosensitizers localize in the endometrium following systemic (Schneider *et al* 1988, Manyak *et al* 1989, Petrucco *et al* 1990, Bhatta *et al* 1992) or topical application (Chapman *et al* 1993, Yang *et al* 1993, Wyss *et al* 1994) and that enduring photodynamic destruction is feasible. Assuming that sufficient photosensitizing drug can be placed in critical endometrial structures, we designed the present study to explore issues associated with uterine light dosimetry that ultimately determine the extent of photodynamic destruction.

We and others have shown that light must be distributed throughout the endometrial layer in order to cause irreversible destruction (Steiner *et al* 1995, Wyss *et al* 1994, 1995). The human endometrium has unique proliferation and neovascularization characteristics which dictate light and drug dosimetry requirements. Depending on the phase of the menstrual cycle, its thickness varies between 2 and 5 mm (Gonen *et al* 1989). Optimization of uterine PDT therefore requires development of a minimally invasive light delivery system that can provide an applied light dose (total fluence) throughout the endometrium which exceeds threshold levels for photodynamic destruction.

In this report, we describe an analytical model based on diffusion theory to predict the optical fluence rate in the uterus for cylindrical and spherical optical applicators. Model predictions are used to estimate the thermal effects of optical irradiation and the effective photodynamic dose at a given tissue depth. Theoretical fluence rate calculations are compared to fluence rate measurements made in fresh, surgically removed human uteri. We conclude that a trifurcated, cylindrical optical applicator inserted into the human uterus is an effective system for irradiating the entire endometrium. This intrauterine delivery system can provide an adequate dose for complete photodynamic destruction in a reasonable time period using moderate light intensities.

2. Theory

2.1. Optical distribution

For most PDT applications, maintaining a sufficiently high light dose in the region between targeted and surrounding normal tissue, e.g. at tumour margins, is critical to clinical outcome. Red/near-infrared light reaching these regions will usually have undergone multiple scattering and the optical radiance will therefore be almost isotropically distributed. The spatial distribution of the optical fluence rate can then be adequately described by the diffusion approximation of the more general equation of radiative transfer (Ishimaru 1978, Svaasand 1984, Profio and Doiron 1987). Provided that the proper boundary condition is used at the source–tissue interface, this approximation will give a good description of the fluence rate somewhat distal to the source. However, the diffusion approximation clearly breaks down with increasing proximity to the source. In cases where light is coupled into the tissue by embedded diffusing applicators (e.g. spherical or cylindrical diffusing fibres) rather than by collimated beams, the diffusion approximation might be very good even close to the source–tissue interface. Since we are primarily interested in estimating fluence rate distributions several millimetres from diffusing applicators (regions most critical to clinical

outcome), we expect that the diffusion approximation is valid for most light dosimetry problems in uterine PDT.

The diffusion approximation can be expressed in terms of two equations: a driving force equation and a conservation equation. The driving force equation can be expressed in the same manner as in Fick's law,

$$\boldsymbol{j} = -(D/c)\,\mathrm{grad}\,\varphi \tag{1}$$

where $\boldsymbol{j}$ and φ are, respectively, the diffuse photon flux vector and the optical fluence rate. The velocity of light c is given by $c = c_0/n$ where c_0 is the velocity of light in vacuum and n is the index of refraction. The quantity D is the optical diffusivity. This quantity can be expressed in terms of the optical absorption and scattering coefficients,

$$D = c/3(\mu_\mathrm{a} + (1-g)\mu_\mathrm{s}) = c/3(\mu_\mathrm{a} + \mu_\mathrm{s}^1) \tag{2}$$

where μ_a and μ_s are, respectively, the optical absorption coefficient and the optical scattering coefficient. The parameter g is the average cosine of the scattering angle and the quantity $\mu_\mathrm{s}^1 = (1-g)\mu_\mathrm{s}$ is the reduced scattering coefficient. The conservation equation can correspondingly be expressed,

$$\mathrm{div}\,\boldsymbol{j} = -\mu_\mathrm{a}\varphi + q \tag{3}$$

where q is the diffuse photon source density.

The two equations combine to give

$$\nabla^2\varphi - \varphi/\delta^2 = -(q/D)c \tag{4}$$

where the optical penetration depth is given by $\delta = \sqrt{D/c\mu_\mathrm{a}}$.

2.2. Cylindrical applicators

The expression for fluence rate in the cylindrically symmetric case where a long cylindrical applicator is positioned coaxially in a uterine cavity, for example, in the murine uterine horn, as shown schematically in figure 1, follows from equation (4). The solution of the homogeneous form of the equation can be expressed (Svaasand 1984) as

$$\varphi = \varphi_0 K_0(r/\delta) \tag{5}$$

where r is the distance from the axis, φ_0 is the fluence rate at the inner surface and K_0 is the modified Bessel K function of zero order.

The flux of light into the medium can then be expressed by the radial component of grad(φ), equation (1)

$$j = -(D/c)(\mathrm{d}/\mathrm{d}r)\varphi = (D/c\delta)K_1(r/\delta)\varphi_0 \tag{6}$$

where K_1 is the modified Bessel K function of first order.

Multiple reflections will build up the fluence rate in the cavity until the radiation transmitted through the cavity wall is equal to the light coupled into the cavity. A relationship between the optical power coupled into the cavity and the optical fluence rate can be obtained by taking the photon flux vector at the surface of the cavity as equal to the direct unscattered irradiation from the applicator. The fluence rate can thus be expressed via equations (5) and (6)

$$\varphi = [P\delta c/2\pi a D K_1(a/\delta)]K_0(r/\delta) \tag{7}$$

where P is the optical power per unit length of the applicator and a is the radius of the cylindrical cavity. The ratio between the actual fluence rate in the inner layer of the lumen

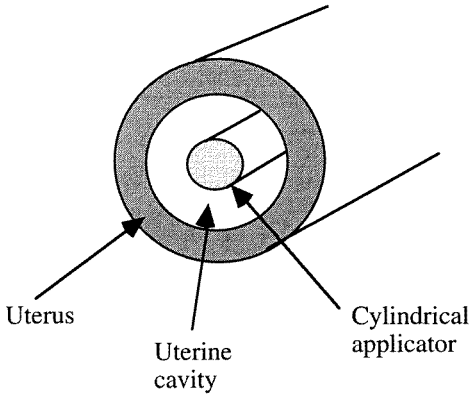

Figure 1. An applicator installed coaxially in a uterine cavity of cylindrical geometry.

wall and the incident unscattered radiation can be expressed in terms of a dimensionless coupling parameter, k_c, that describes the fluence rate in the uterine wall relative to the unscattered incident radiation from the applicator:

$$\varphi(r = a) = k_c P/2\pi a \tag{8}$$

$$k_c = (\delta c/D)K_0(a/\delta)/K_1(a/\delta) \Rightarrow_{a \gg \delta} \delta c/D. \tag{9}$$

This coupling factor increases with the ratio between the radius of the lumen (or with the radius of the applicator for applicators embedded in the tissue) and the optical penetration depth of the tissue, The value of the coupling parameter in the case of a typical size cylindrical applicator of 1.2 mm diameter embedded in the uterine cavity is about 2.7 for an optical penetration depth and diffusivity of, respectively, 2.6 mm and 8.1×10^4 m^2 s^{-1}. The actual fluence rate in the tissue at the interface with the applicator is thus 2.7 times larger than the unscattered light flux emitted by the applicator. This value increases with radius to a maximum value of 6.9 when the radius is much larger than the optical penetration depth. The values of the coupling coefficient given by equation (8) represent, however, an upper estimate of the coupling; any highly absorbing layer on the lumen wall or on the applicator surface will reduce this value.

An example for the optical distribution in tissue is shown in figure 2. This graph gives the optical fluence rate and the corresponding optical dose after 20 min of exposure versus distance from the applicator axis.

2.3. Thermal effects

Optical irradiation will initiate a temperature rise in tissue. This temperature rise will increase during irradiation and will typically reach a steady-state value after about 5 min of exposure (Svaasand *et al* 1989). This steady-state temperature should be kept below about 45 °C if hyperthermic reactions, pain and thermal necrosis are to be avoided. Although a moderate temperature rise to about 42–45 °C might be beneficial by synergistically enhancing photodynamic therapy (Kimel *et al* 1992, Mang 1990), this effect is beyond the scope of this work and is not be considered in the present model. Rather, our mathematical modelling of thermal distributions is restricted to a simplified analysis that focuses on determining the maximum temperature rise in an effort to describe irradiation conditions that would limit this effect to less than about 10 °C.

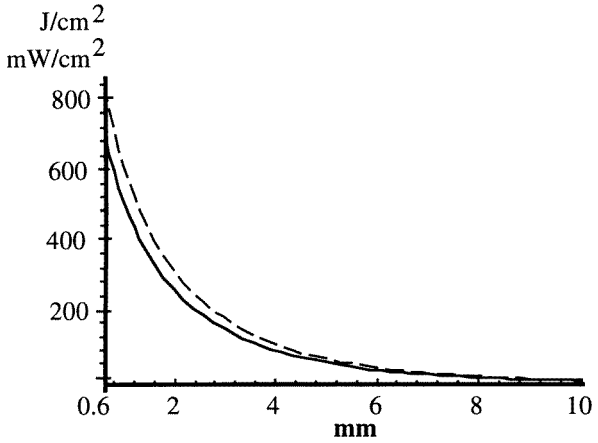

Figure 2. Upper dashed curve, optical dose (J cm^{-2}); lower solid curve, optical fluence rate (mW cm^{-2}) versus distance from applicator axis (mm) for uterus with optical penetration depth, $\delta = 2.6$ mm, optical diffusivity, $D = 8.1 \times 10^4$ m^2 s^{-1}, applicator diameter, 1.2 mm, exposure time, 20 min and power, 100 mW cm^{-1}.

The steady-state temperature distribution can be found from the bioheat equation (Svaasand 1984)

$$\nabla^2 T - T/\delta_v^2 = -q_t/\kappa \tag{10}$$

where T is the temperature rise, q_t is the heat source density and κ is the thermal conductivity. The thermal penetration depth in blood perfused media is given by $\delta_v = \sqrt{\chi/q}$ where χ is the thermal diffusivity and Q is the blood perfusion rate in volume of blood per unit volume of tissue per unit time.

An estimate of the temperature distribution can easily be found by assuming that all the incident light is either absorbed in the lumen wall or absorbed at a depth corresponding to the optical penetration depth. The first condition corresponds to a worst-case scenario that might occur if a blood clot is formed at the applicator surface since clot formation might result in a blackish layer that absorbs practically all light. The second condition is more desirable since all light is absorbed within the tissue itself.

The temperature distribution in the case where all light is absorbed at a distance b from the applicator axis is given by

$$T = [P\delta_v/2\pi b\kappa K_1(b/\delta_v)]K_0(r/\delta_v). \tag{11}$$

The maximum temperature rise that will occur at a depth equal to b is illustrated in figure 3 for a delivered power of 100 mW cm^{-1} length of the applicator. The thermal conductivity and diffusivity are, respectively, $\kappa = 0.6$ W m^{-1} K^{-1} and $\chi = 1.4 \times 10^{-7}$ m^2 s^{-1}. The temperature rise is calculated for two values of the thermal penetration depth, i.e., $\delta_v = 3.2$ mm and $\delta_v = 10$ mm, as indicated by the dashed and solid lines in figure 3, respectively. The value of 3.2 mm corresponds to a high perfusion rate, i.e., 50 ml per minute through a uterus of weight 0.060 kg, whereas the 10 mm thermal penetration depth corresponds to a comparatively low blood perfusion rate of 8.4 ml per minute per 100 g tissue.

This graph demonstrates that a delivered power of 100 mW cm^{-1} from a 0.6 mm radius applicator is expected to initiate a worst-case temperature rise of about 10–11 °C. Provided that clot formation at the applicator-tissue interface is avoided and light is absorbed

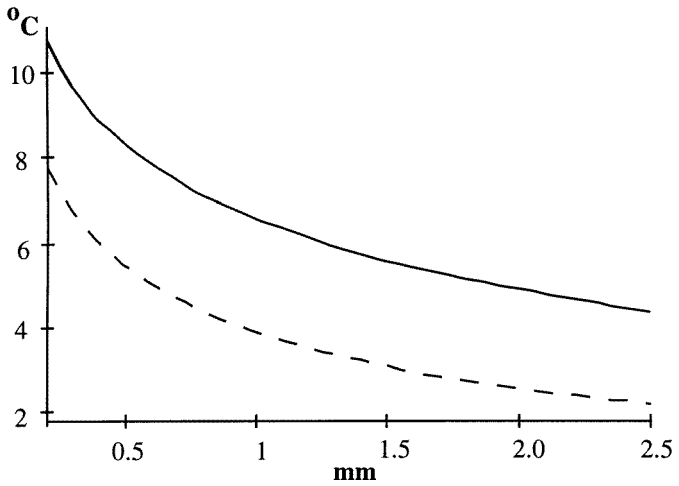

Figure 3. Calculated maximum temperature rise versus depth of absorption of optical power for two different thermal penetration depths. Upper solid curve, thermal penetration depth $\delta_v = 10$ mm; lower dashed curve, $\delta_v = 3.2$ mm. Thermal diffusivity, $\kappa = 0.6$ W m^{-1} K^{-1}, power, 100 mW cm^{-1}; applicator diameter, 1.2 mm.

within the optical penetration depth, the temperature rise should be below about 6 °C. As a result, under normal conditions with reasonable perfusion, 100–200 mW cm^{-1} are probably acceptable power levels. However, delivered powers in the 200 mW cm^{-1} range should only be used in tissues with high optical penetration depths and high blood perfusion rates. Since it is generally accepted that PDT-induced physiological changes can reduce blood flow, these values clearly represent upper-limit exposure estimates.

2.4. Spherical applicators

The optical distribution in the case where an isotropic applicator is positioned centrally in a spherical cavity can be expressed using equation (4).

$$\varphi = \varphi_0 \mathrm{e}^{-r/\delta}/r \tag{12}$$

where r is the distance from the centre and φ_0 is the fluence rate at the inner surface of the cavity.

The flux of light into the medium can then be expressed using equation (1).

$$j = -(D/c)(\mathrm{d}/\mathrm{d}r)\varphi = (D/rc)(1/r + 1/\delta)\mathrm{e}^{-r/\delta}\varphi_0. \tag{13}$$

Multiple reflections will build up the fluence rate in the cavity until the radiation transmitted through the cavity wall is equal to the light coupled into the cavity. The fluence rate can thus be expressed

$$\varphi = [P_t c/4\pi a D r(1/a + 1/\delta)]\mathrm{e}^{-(r-a)/\delta} \tag{14}$$

where P_t is the total optical power from the applicator.

The ratio between the actual fluence rate in the inner layer of the cavity wall and the incident unscattered radiation can be expressed

$$\varphi(r = a) = k_\mathrm{s} P_t/4\pi a^2 \tag{15}$$

where

$$k_\mathrm{s} = (\delta c/D)a/(a + \delta) \Rightarrow_{a \gg \delta} \delta c/D.$$

An estimate of the maximum temperature rise for a spherical applicator embedded in the tissue can be obtained by assuming that all the incident light is absorbed at a distance b from the applicator centre. The maximum temperature rise can thus be expressed

$$T_{max} = P_t/4\pi b^2 \kappa (1/b + 1/\delta_v). \tag{16}$$

Typically, an incident power of 100 mW at 630 nm from a 0.4 mm radius spherical applicator may initiate a worst-case temperature rise of about 30 °C, but the temperature rise will be below 5 °C under more normal conditions.

2.5. Effective optical dose

The sensitizer will photodecompose during irradiation. The concentration, C, after irradiation by an optical fluence Ψ can be expressed (Grossweiner 1991)

$$C = C_0 \mathrm{e}^{-\Psi/\Theta} \tag{17}$$

where C_0 is the initial photosensitizer concentration. The bleaching effect is characterized by the bleaching parameter Θ that describes the amount of optical fluence required to photobleach the drug concentration to 1/e, i.e., to 37% of the initial concentration. When light is absorbed by the photosensitizer, toxic oxygen species (e.g., singlet oxygen) are generated which irreversibly oxidize (damage) tissue components (e.g., cells and organelles). Singlet oxygen generation is, therefore, fundamental to the process of tissue destruction. For an infinitesimally small optical dose, $\mathrm{d}\Psi$, singlet oxygen is produced in an amount, $\mathrm{d}Q$, which is proportional to photosensitizer concentration, C, and the quantum efficiency of the process, k:

$$\mathrm{d}Q = kC\,\mathrm{d}\Psi. \tag{18}$$

The total amount of singlet oxygen, Q, generated by a total optical dose Ψ can thus be determined by

$$Q = \int_0^{\Psi} kC\,\mathrm{d}\Psi = \int_0^{\Psi} kC_0 \mathrm{e}^{-\Psi/\Theta}\,\mathrm{d}\Psi = kC_0\Theta(1 - \mathrm{e}^{-\Psi/\Theta}) \tag{19}$$

which enables the definition of an effective optical dose

$$\Psi_{\mathrm{eff}} = \Theta(1 - \mathrm{e}^{-\Psi/\Theta}). \tag{20}$$

The relationship between the optical dose and the *effective* optical dose is illustrated in figure 4. The upper curve in this graph corresponds to the same optical dose as shown in figure 2, whereas the lower curve corresponds to the effective dose. The lower curve is valid for a bleaching fluence of 75 J cm^{-2} corresponding to that of the commonly used photosensitizer haematoporphyrin derivative (HpD) (Svaasand and Potter 1992). Measurements of human basal cell carcinomas using another frequently used photosensitizer, topically applied 5-aminolevulinic acid (5-ALA), yielded protoporphyrin IX (PpIX) bleaching fluences in the range of 30–50 J cm^{-2} (Hoeydalsvik 1994). These simulations clearly demonstrate that, in the region close to the applicator where Ψ is usually much greater than Θ, the bleaching process limits the effective dose to $\Psi_{eff} \approx \Theta$. However, photobleaching is obviously of minor importance far from the source where, at the margins of the treated tissue, Ψ is typically less than Θ.

Finally, it should be noted that the presented concept of an effective dose is only applicable in the case of uniform sensitizer distribution in the target tissue. This criterion is presumed to be satisfied with systemically injected sensitizers and may not always be valid in the case of topically administered drug. In addition, the actual cytotoxic dose

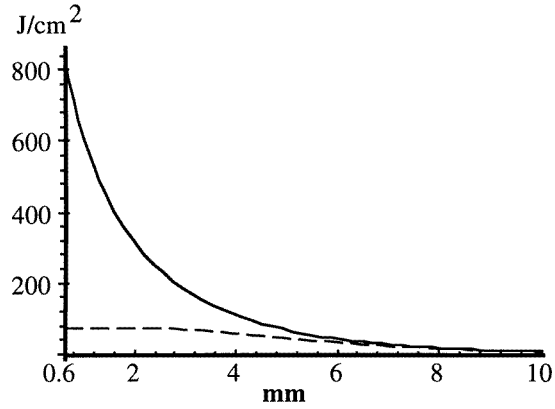

Figure 4. Calculated optical dose and effective optical dose (J cm^{-2}) versus distance from applicator axis (mm). Upper curve, applied optical dose; lower curve, effective optical dose for bleaching parameter, $\Theta = 75$ J cm^{-2}. Optical penetration depth, $\delta = 2.6$ mm; optical diffusivity, $D = 8.1 \times 10^4$ m^2 s^{-1}; applicator diameter, 1.2 mm; exposure time, 20 min; power, 100 mW cm^{-1}.

can be different from the effective dose since it depends on parameters such as drug concentration, drug localization within the cell, and the fluence-rate-dependent oxygen depletion. Nevertheless, these results underscore the importance of photobleaching, since even accurately calculated *in situ* light doses could provide overoptimistic estimates of tissue damage. This is particularly important for uterine PDT since it requires sufficiently high light doses to alter tissue at depths of about 2–6 mm, regions that can obviously be quite sensitive to the bleaching process.

3. Methods and materials

3.1. Uterus measurements

The dosimetry model was tested by measuring the light distribution from cylindrical fibres in three different premenopausal human uteri. All measurements were completed within 2–4 h of hysterectomy. In order to maintain the properties of the excised specimens as close as possible to the *in vivo* situation, all major vessels of the uterus were closed by sutures just prior to hysterectomy. Specimens were placed on ice and measurements were initiated within 45 min of removal. A cylindrical fibre applicator (source fibre) was inserted through the cervix and an isotropic detector fibre was inserted through the uterine wall. A channel for the detector fibre was made by the insertion of a hypodermic needle. The needle was retracted and the detector fibre was inserted in the channel. The initial positioning of the detector fibre with respect to the cylindrical applicator was visually verified with the use of a 3 mm rigid hysteroscope. The detector fibre was then retracted in a direction normal to the axis of the cylinder, and the positioning was monitored by micrometer readings. The detector fibre was positioned in the endometrial layer over the first 3–4 mm. Larger source–detector separations corresponded to placement of the detector fibre in the myometrial layer. The lumen of the uterine cavity was collapsed during the measurements. The dimensions of the cylindrical diffusing fibres were 1.2 mm in diameter and 30 mm in length, and the diameter of the spherical probe was 0.8 mm (PDT Systems, Inc, Santa Barbara, CA). The spherical detector fibre was calibrated by immersing the tip into a water-filled cuvette (in order to

simulate the refractive index of tissue) and irradiating with an He:Ne laser beam focused to a spot of diameter less than that of the detector tip. The distal end of the detector fibre was directed onto a photomultiplier tube (R928, Hamamatsu Corp.) and photocurrent levels were recorded as a function of laser power for various photomultiplier gain and high voltage settings. The 633 nm He:Ne beam power was measured prior to each probe calibration using an independently calibrated thermopile detector (model 1815c, Newport Corporation, Irvine, CA). The variation in calibration when the beam was coupled to the sphere from different directions was $\pm 10\%$. For tissue studies, a total of 300 mW (100 mW cm^{-1} diffusing tip) of 630 nm light provided by an argon-ion-pumped dye laser (Coherent Innova 90-5/599 argon-dye system with DCM dye) was launched into the 3 cm long cylindrical source fibre.

4. Results and discussion

The cavity of the human uterus is normally collapsed and has a triangular shape. Several cylindrical applicators will therefore usually be required in order to deliver a sufficiently uniform optical dose through the uterine cavity into the endometrium. A possible construction of such a composite applicator is outlined in figure 5. The applicator consists of three individual cylindrical fibres that can be spread out in a trifurcation after insertion into the uterine cavity. The uterine wall is assumed to be in full contact with the applicator. Each fibre is positioned in the x–y plane illustrated in figure 5(B). The length of the central fibre is about 30–40 mm and the angle between neighbouring fibres is in the range of 0.25–0.40 rad.

The effective optical dose (J cm^{-2}) from this applicator is shown in figure 6 for three different treatment planes (lower, middle and upper fundal) which, as shown in figure 5(B), are perpendicular to the treatment fibres and positioned in the x–z plane. The left-hand horizontal axes in figure 6 provide the distance from the middle fibre, perpendicular to the x–y plane, along the z axis of figure 5(B). The right-hand horizontal axes give the corresponding distance from the middle fibre in a direction parallel to the x–y plane, i.e. along the x axis of figure 5(B). Figure 6(A)–(C) shows the effective optical dose (from (20)) in the lower, middle and upper fundal treatment planes, respectively. Each part ((A)–(C)) thus provides information on a quarter segment of the x–z plane of figure 5(B).

The length of the central applicator in the calculations is assumed to be 40 mm, the diameter of each applicator is 1.2 mm and the angle between two neighbouring applicators is 0.25 rad (14°). The optical power is 100 mW cm^{-1} i.e., 100 mW per cm of each individual cylinder, the exposure time is 20 min and the bleaching fluence is 75 J cm^{-2}. The optical penetration depth is assumed to be in the lower range of the published values, i.e., $\delta = 2.6$ mm and the diffusivity, $D = 8.1 \times 10^4$ m^2 s^{-1}.

The minimum fluence rate is found in the upper fundal plane because the distances between the fibres are greatest here and because each fibre may be assumed to act as a semi-infinite long cylinder. An intermediate value is found in the middle plane where all fibres act as infinitely long cylinders, and the maximum value is found in the lower isthmic plane where three semi-infinite cylinders join. These data clearly show that a satisfactory *in situ* optical dose of approximately 50 J cm^{-2} can be delivered at a reasonable depth in the difficult-to-treat upper fundal plane. Although the 20 min irradiation period just manages to provide the minimum required light dose throughout the endometrium, it is important to point out that these simulations are based on 'worst-case' optical properties ($\delta = 2.6$ mm). We have generally observed penetration depths on the order of about 4 mm for premenopausal uteri (Madsen *et al* 1994a, b) and consequently expect sufficiently high light levels to be easily achievable in a 15–20 min timeframe for most patients. However,

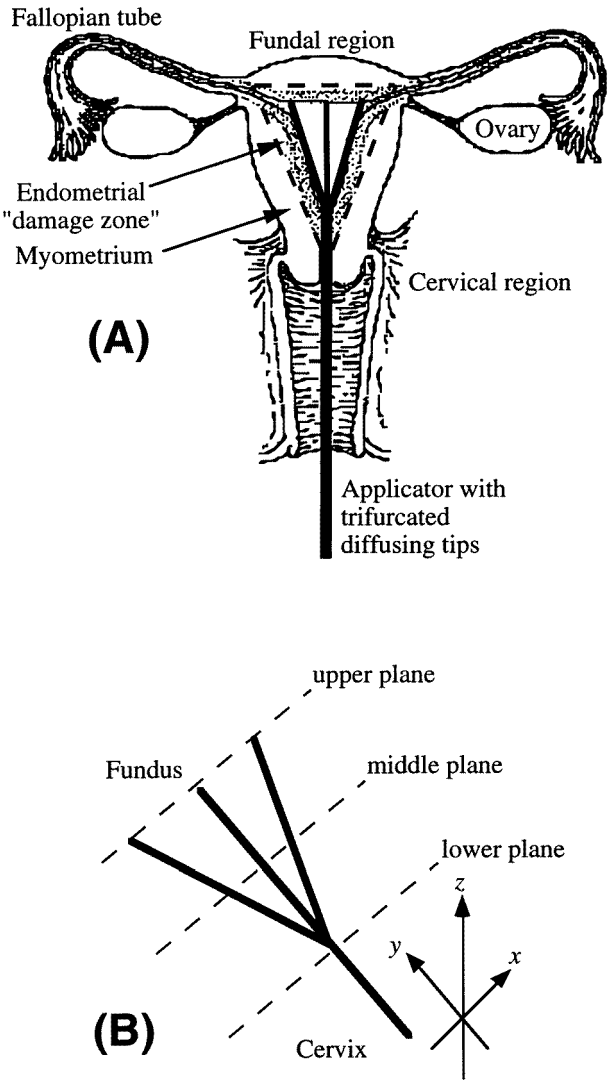

Figure 5. (A) A human uterus with inserted applicator illustrating three cylindrical diffusing fibres positioned in the lumen; (B) the location of three coplanar cylindrical fibres in the x–y plane with respect to x–z fundal, middle and lower treatment planes.

the precise light dose required for photodynamically altering endometrial structure and function is not known. Accurate knowledge of light dose damage thresholds combined with individual patient measurements of endometrial structural and optical properties could be used to adjust the applied light dose to achieve the desired tissue response.

The correlation between actual light distribution measurements and calculated values is shown for two different uteri in figure 7. The solid lines in the figure correspond to the predicted fluence rate (from equation (7)) in the case of an infinitely long 1.2 mm diameter cylindrical diffusing fibre with an emitted optical power of 100 mW cm^{-1}. The optical properties used in the calculated response were determined from the measured penetration depths ((A) $\delta = 4.0$ mm; (B) $\delta = 4.4$ mm) and diffusivities, $D = 9.6 \times 10^4$ m^2 s^{-1}

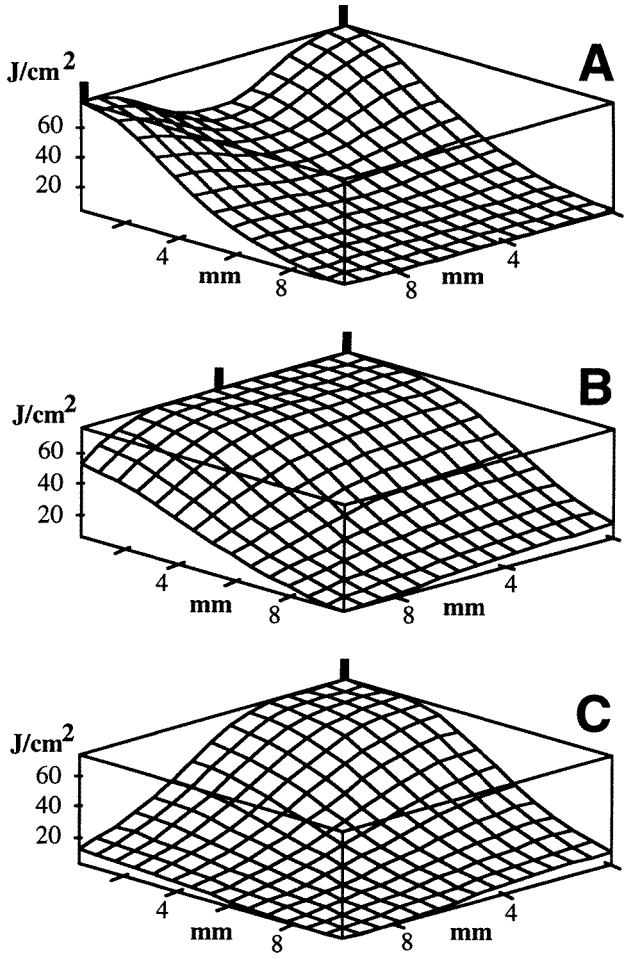

Figure 6. The calculated effective optical dose for $\delta = 2.6$ mm, $D = 8.1 \times 10^4$ m^2 s^{-1}, applicator diameter, 1.2 mm, exposure time, 20 min, power, 100 mW cm^{-1} and $\Theta = 75$ J cm^{-2}: (A) lower treatment plane; (B) middle treatment plane; (C) upper fundal plane. Left-hand horizontal axes show the distance (mm) from the middle fibre along the z axis, perpendicular to the x–y plane of figure 5(B). Right-hand horizontal axes show the distance from the middle fibre along the x axis, parallel to the x–y plane of figure 5(B). Fibre positions are indicated by solid vertical lines on top of each panel; the central fibre is located in the centre of each figure.

(upper line) and 8.1×10^4 m^2 s^{-1} (lower line) taken from our previously published values for premenopausal human uteri at 630 nm (Madsen *et al* 1994a, b). Measurements were performed by launching 630 nm light (100 mW cm^{-1} diffusing tip) from the argon-ion-pumped dye laser onto a 1.2 mm diameter, 30 mm long cylindrical diffusing fibre placed inside the collapsed uterine cavity. Data points represent absolute fluence rate measurements obtained using the precalibrated, 0.8 mm diameter isotropic detector fibre inserted through the uterine wall.

These results highlight two important points. First, both (A) and (B) show reasonable agreement between measured and calculated fluence rates, particularly in deep tissue regions where it is critical to have a sufficiently high optical dose to initiate PDT. This provides preliminary validation of our light distribution model and permits its utilization in human

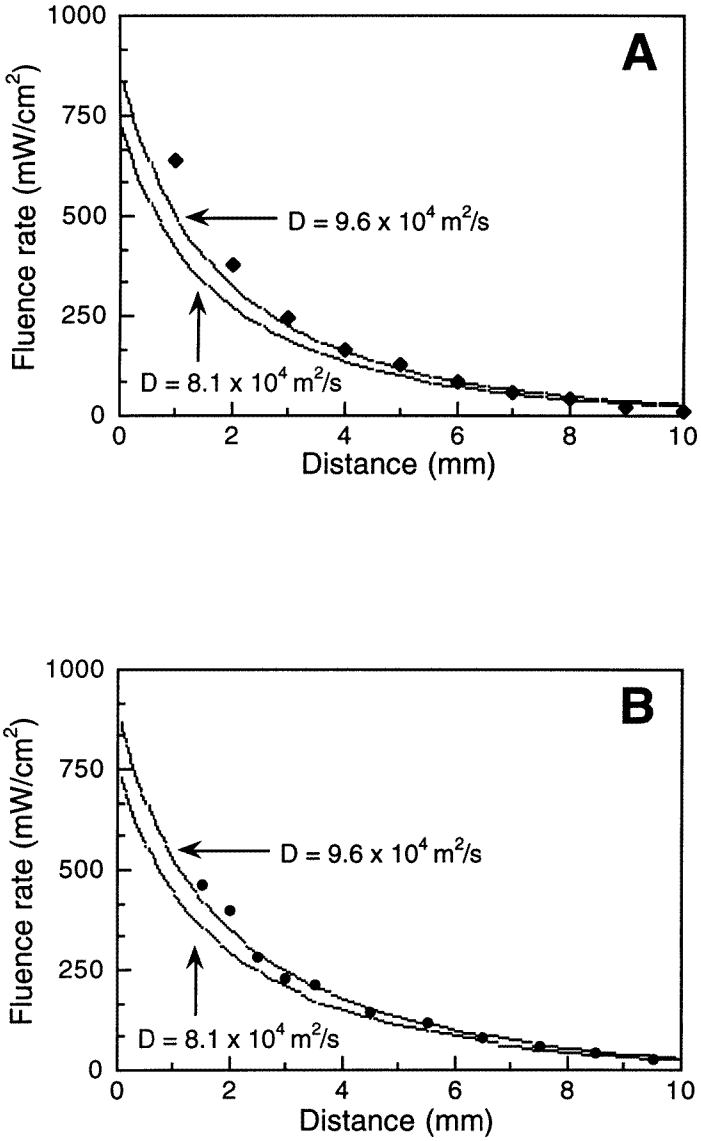

Figure 7. Measured and calculated fluence rate (mW cm^{-2}) versus distance (mm) from a single cylindrical applicator axis for premenopausal human uteri. (A) Optical penetration depth, $\delta = 4$ mm, ♦, measured data points; (B) $\delta = 4.4$ mm, ●, measured data points; (A) and (B) smooth lines, simulated response, from equation (7), for two different optical diffusivities, D: 9.6×10^4 m^2 s^{-1} (upper line) and 8.1×10^4 m^2 s^{-1} (lower line). Measurements and simulations show the response in the midplane of a 1.2 mm diameter, 3 cm long diffusing fibre at 100 mW cm^{-1}, $\lambda = 630$ nm.

dosimetry applications. Second, since each figure 7 simulation was performed at fixed δ values, deviations between measured and predicted fluence rates, most noticeable at $D = 8.1 \times 10^4$ m^2 s^{-1}, are due to changes in tissue scattering properties (as suggested by equation (9)). Thus, knowledge of the penetration depth alone may not be sufficient for successfully predicting PDT light dosimetry. More accurate optical dose estimates could be

obtained by measuring μ_a and μ_s' prior to treatment using a technique such as frequency-domain photon migration (FDPM) (Tromberg *et al* 1995).

The most critical location for obtaining an adequate fluence rate is in the region where the distances between the fibres are maximal, i.e., between the fibres in the fundal zone (see figure 5). The fluence rate in this area can, however, be significantly improved if the uterine walls are separated by a few millimetres. This was experimentally verified in a set-up where all three fibres were radiating. The fluence rate was monitored in the critical region, 2–4 mm from the uterine wall, when 3–5 ml of a high-viscosity, optically clear liquid (Hyskon^{TM}, Pharmacia Inc., Piscataway, NJ) was injected into the uterine cavity. The fluence rate increased typically by a factor of six to 10 after the injection. A rough estimate for the light distribution in this case can be found by considering the uterine lumen as an optically integrating cavity limited by parallel triangular planes. The light distribution is then given by equations (1) and (3)

$$\varphi \approx (3Pl/2\delta\mu_a l_f l_{cf})\mathrm{e}^{-x/\delta} \tag{21}$$

where l is the applicator length, l_f is the length along the uterine fundus, l_{cf} is the distance from the cervix to the fundus and x is the distance from the wall. The factor of two in the denominator accounts for the 'semi-infinite' extent of the plane in this region.

The agreement between the observed increase in optical fluence by a factor of six to ten in the region between the fibres, and the estimated value of six to nine indicates that the build up of fluence rate in the uterine cavity from light scattered back from the uterine wall is a very efficient process (van Staveren *et al* 1994).

5. Conclusions

We have presented an analytical model for estimating the optical fluence rate in human uteri using a trifurcated, cylindrical fibre applicator. Model predictions for a cylindrical fibre source are in good agreement with actual fluence rate measurements conducted in freshly excised human uteri. Major uterine blood vessels were clamped during surgery and the measured optical properties are therefore expected to be close to the *in vivo* situation. Since the absorbance of photosensitizer, e.g. porphyrins, is generally negligible compared to intrinsic tissue chromophores, the measured uterine properties should be close to the values during treatment. Although these tissue parameters can be used as a general guide for PDT dosimetry, optical property measurements can be performed following drug administration and irradiation using techniques such as frequency-domain photon migration. This will make it possible to observe small tissue absorption and scattering changes during therapy that may impact light and drug dosimetry (Tromberg *et al* 1995).

When 100 mW cm^{-1} is launched down each 3 cm arm of the applicator, we estimate that 50 J cm^{-2} can be delivered at a depth of 4–6 mm in 20 min or less. Although the actual light dose in a given patient depends on individual uterine optical properties, our model calculations are determined using published 1/e optical penetration depths (δ) which range from 2.6 to 4.5 cm. Interestingly, a sixfold to 10-fold increase in fluence rate at a given depth can be observed by distending the lumen with an optically transparent medium which effectively turns the cavity into an 'integrating sphere'. We conclude that the trifurcated light applicator described herein can generate an optical dose that is adequate for destruction of the entire endometrium in a reasonable time period, provided tissue photosensitivity is comparable to that reported for photodynamic treatment of tumours with systemically injected Photofrin. The actual tissue response and degree of regeneration for a given patient

ultimately depend on photodynamic damage parameters which must be explicitly determined for a given photosensitizer and administration route.

Acknowledgments

This work was supported by the National Institutes of Health (NIH No R29GM50958) and the Whitaker Foundation (WF16493). In addition, Beckman Laser Institute programmatic support was provided from the National Institutes of Health (NIH No 5P41RR01192-15), the Department of Energy (DOE No DE-FG03-91ER61227) and the Office of Naval Research (ONR No N00014-91-C-0134). MKF wishes to acknowledge fellowship assistance from the Swiss National Science Foundation.

References

Bhatta N, Anderson R, Flotte T, Schiff I, Hasan T and Nishioka N S 1992 Endometrial ablation by means of photodynamic therapy with Photofrin II *Am. J. Obstet. Gynecol.* **167** 1856–63

Brooks P G and Serden S P 1991 Hormonal inhibition of the endometrium for retroscopic endometrial ablation *Am. J. Obstet. Gynecol.* **164** 1601

Chapman J A, Tadir Y, Tromberg B J, Yu K, Manetta A, Sun C-H and Berns M W 1993 Effect of administration route and estrogen manipulation on endometrial uptake of Photofrin *Am. J. Obstet. Gynecol.* **168** 685–92

Daniell J F, Kurtz B R and Ke R W 1992 Hysteroscopic endometrial ablation using the rollerball electrode *Obstet. Gynecol.* **80** 329–32

DeCherney A and Polan M L 1983 Hysteroscopic resection of intrauterine lesions and intractable uterine bleeding *Obstet. Gynecol.* **61** 392–7

Goldrath M H, Fuller T A and Segal S 1981 Laser photovaporization of endometrium for treatment of menorrhagia *Am. J. Obstet. Gynecol.* **140** 14–19

Gonen Y, Casper R F, Jacobson W and Blankier J 1989 Endometrial thickness and growth during ovarian stimulation: a possible predictor of implantation in vitro fertilization *Fert. Steril.* **52** 446–50

Grossweiner L I 1991 Light dosimetry for photodynamic therapy treatment planning *Lasers Surg. Med.* **11** 165–73

Hoeydalsvik E 1994 Characterization of the distribution of porphyrins in malignant tumors by fluorescence *MSc Thesis* Division of Physical Electronics, Norwegian Institute of Technology

Ishimaru A 1978 *Wave Propagation and Scattering in Random Media* (New York: Academic)

Jedeikin R, Olsfanger D and Kessler I 1990 Disseminated intravascular coagulopathy and adult respiratory distress syndrome: life-threatening complications of hysterscopy *Am. J. Obstet. Gynecol.* **162** 44–5

Kimel S, Svaasand L O, Hammer-Wilson M, Gottried V, Cheng S, Svaasand E and Berns M W 1992 Demonstration of synergistic effects of hyperthermia and photodynamic therapy using the chick chorioallantoic membrane model *Lasers Surg. Med.* **12** 432–40

Lynne S W, Koonin L M, Pokras R, Strauss L T, Xia Z and Peterson H B 1994 Hysterectomy in the United States, 1988–1990 *Obstet. Gynecol.* **83** 549–55

Madsen S J, Tromberg B J, Wyss P, Svaasand L O, Haskell R C and Tadir Y 1994a The optical properties of human uterus at 630 nm *Advances in Optical Imaging and Photon Migration, Proc. Opt. Soc. Am. (Orlando, FL, 1994)* vol 21 (Washington, DC: Optical Society of America) pp 262–4

Madsen S J, Wyss P, Svaasand L O, Haskell R C, Tadir Y and Tromberg B J 1994b Determination of the optical properties of human uterus using frequency-domain photon migration and steady-state techniques *Phys. Med. Biol.* **39** 1191–202

Mang T S 1990 Combination studies of hyperthermia induced by the neodymium–yttrium-aluminium-garnet (Nd–YAG) laser as an adjuvant to photodynamic theory *Lasers Surg. Med.* **10** 173–8

Manyak M J, Nelson L M and Solomon D 1989 Photodynamic therapy of rabbit endometrium transplants: a model for treatment of endometriosis *Fert. Steril.* **52** 140–5

Perry P M and Baughman V L 1990 A complication of hysteroscopy: air embolism *Anesthesiology* **73** 546–7

Petrucco O M, Sathananden M, Petrucco M F *et al* 1990 Ablation of endometriotic implants in rabbits by hematoporphyrin derivative photoradiation therapy using the gold vapor laser *Lasers Surg. Med.* **10** 344–8

Profio A E and Doiron D R 1987 Transport of light in tissue in photodynamic therapy *Photochem. Photobiol.* **46** 591–9

Schneider D, Schellhas H F, Wessler T A *et al* 1988 Endometrial ablation by DHE photoradiation therapy in estrogen treated ovariectomized rats *Colposc. Gynecol. Laser Surg.* **4** 73–7

Serden S P and Brooks P G 1991 Treatment of abnormal uterine bleeding with the gynecologic resectoscope *J. Reprod. Med.* **36** 697

Steiner R A, Tromberg B J, Wyss P, Krasieva T, Chandanani N, McCullough J, Berns M W and Tadir Y 1995 Rat reproductive performance following photodynamic therapy with topically-administered photofrin *Human Reprod.* **10** 227–33

Svaasand L O 1984 Optical dosimetry for direct and interstitial photoradiation therapy of malignant tumors *Porphyrin Localization and Treatment of Tumors* ed D Doiron and C Gomer (New York: Liss) pp 91–114

Svaasand L O, Gomer C J and Profio A E 1989 Laser induced hyperthermia of ocular tumors *Appl. Opt.* **28** 2280–7

Svaasand L O and Potter W 1992 The implications of photobleaching for photodynamic therapy *Photodynamic Therapy: Basic Principles and Clinical Aspects* ed B Henderson and T J Dougherty (New York: Dekker) pp 369–84

Tromberg B J, Haskell R C, Madsen S J and Svaasand L O 1995 Characterization of tissue optical properties using proton density waves *Comment. Mol. Cell. Biophys.* **8** 359–86

van Staveren H J, Beek J F, Ramaekers J W H and Keijzer M 1994 Integrating sphere effect in whole bladder wall photodynamic therapy I. 532 nm verses 630 nm optical irradiation *Phys. Med. Biol.* **39** 947–59

Wyss P, Svaasand L O, Tadir Y, Haller U, Berns M W, Wyss M T and Tromberg B J 1995 Photomedicine of the endometrium: experimental concepts *Human Reprod.* **10** 221–6

Wyss P, Tromberg B J, Wyss M Th, Krasieva T, Schell M, Berns M W and Tadir Y 1994 Photodynamic destruction of endometrial tissue using 5-aminolevulinic acid (5-ALA) in rats and rabbits *Am. J. Obstet. Gynecol.* **171** 1176–83

Yang J Z, Van Vugt D A, Kennedy J C and Reid L R 1993 Evidence of lasting functional destruction of the rat endometrium after 5-aminolevulinic acid-induced photodynamic ablation: prevention of implantation *Am. J. Obstet. Gynecol.* **68** 995–1001